

Parallel Optical Computing Based on MIMO Metasurface Processors with Asymmetric Optical Response

Amirhossein Babae¹, Ali Momeni¹, Ali Abdolali¹, Romain Fleury²

¹*Applied Electromagnetic Laboratory,
School of Electrical Engineering,*

Iran University of Science and Technology, Tehran, Iran

²*Laboratory of Wave Engineering,
Swiss Federal Institute of Technology in Lausanne (EPFL),
CH-1015 Lausanne, Switzerland*

We present a polarization-insensitive metasurface processor to perform spatial asymmetric filtering of an incident optical beam, thereby allowing for real-time parallel optical processing. To enable massive parallel processing, we introduce a novel Multi Input-Multi Output (MIMO) computational metasurface with asymmetric optical response that can perform spatial differentiation on two distinct input signals regardless of their polarization. In our scenario, two distinct signals set in x and y directions, parallel and perpendicular to the incident plane, illuminate simultaneously the metasurface processor, and the resulting differentiated signals are separated from each other via appropriate Spatial Low Pass Filters (SLPF). By leveraging Generalized Sheet Transition Conditions (GSTCs) and surface susceptibility tensors, we design an asymmetric meta-atom augmented with normal susceptibilities to reach asymmetric optical response at normal beam illumination. Proof-of-principle simulations are also reported along with the successful realization of signal processing functions. The proposed metasurface overcomes major shortcomings imposed by previous studies such as large architectures arising from the need of additional subblocks, slow responses, and most importantly, supporting only a single input with a given polarization. Our results set the path for future developments of material-based analog computing using efficient and easy-to-fabricate MIMO processors for compact, fast, and integrable computing elements without any Fourier lens.

I. INTRODUCTION

With the expeditious development of technology in today's communications systems, signal and image processing has gained a lot of attention in the past decade [1–3]. The idea of signal processing by analog computing has been known for a long time, but in the late 20th century, when the digital revolution began, digital computation sat in place of analog computation. Although it was a huge breakthrough, these digital systems suffer from serious restrictions such as data conversion loss and operational speed [4]. Analog solutions therefore emerged again and proved to be advantageous for specific tasks, for example the processing of large size images [5, 6]. Optical signal processing, in particular, largely overcomes the serious limitations of digital systems in term of speed and power consumption [6]. Therefore, designing fast, integrated, and ultra-low power consumption optical devices with high-throughput is one of the key necessities to develop today's modern optical analog processing, and move towards commercial applications with real-time performance.

Spatial optical analog computing based on computational metamaterials is generally based on two major methods: Greens Function (GF) method and metamaterial surfaces (metasurface), with two additional subblocks to apply Fourier and Inverse Fourier Transforms [7–9]. Both approaches, however, suffer from the large final size of the system [5, 7, 8]. Over the past few years, in order to sidestep the drawbacks associated

with the Fourier transform sub-blocks, optical analog computing based on a single metasurface has attracted particular attention as an artificial real-time and high-throughput thin film computer. This allowed migrating from free-space and bulky systems into conceptually subwavelength-sized meta-atoms to perform mathematical operations [10–27]. Metasurfaces that efficiently manipulate the optical wave in the spatial domain are synthesized via several approaches such as GSTCs and susceptibility tensors, which provide an insightful vision for the engineering of meta-atoms with specific angular scattering properties [13, 15, 28–32]. Due to their benefits in terms of low-profile, low sensitivity to absorption losses, and ease of fabrication, metasurfaces are interesting practical alternatives for bulky solutions, especially when it comes to applications including tunable/broadband scattering manipulation [33–41] or antenna engineering [42–45].

In order to be relevant to the widest possible class of signal processing operations, it is momentous that designed optical systems can operate filtering operations on multiple inputs, especially to develop massive parallel-processing schemes. Recently, some proposals have theoretically introduced parallel signal processing for inputs at different angles or two orthogonal polarizations [13, 15, 16]. Although numerous efforts have been made to expand the functionalities of wave-based signal processing systems, a solution allowing for parallel signal processing without the stringent requirements of working at different incidence angles or given polarization states

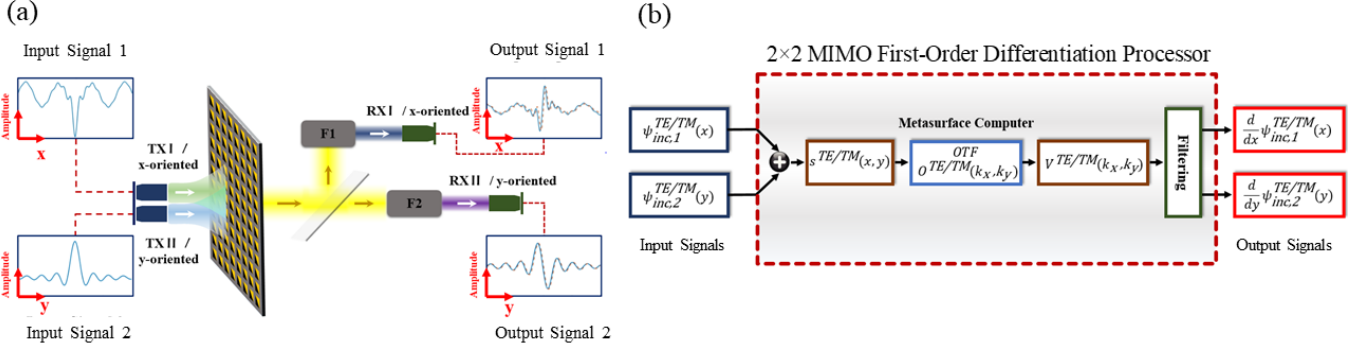


FIG. 1: (a) Schematic sketch of the proposed spatial MIMO metasurface processor for performing real-time parallel optical signal processing. (b) The block diagram of the 2×2 MIMO first-order differentiation processor. Input signal 1, $\psi_{inc,1}^{TE/TM}(x)$, and Input signal 2, $\psi_{inc,2}^{TE/TM}(y)$, have x- and y-variations, respectively. The input signals illuminate normally and simultaneously the metasurface processor and the transmitted waves are separated by F1 and F2 which are spatial low pass filters related to the k_x and k_y directions, respectively. Finally, $\frac{d}{dx}\psi_{inc,1}^{TE/TM}(x)$ and $\frac{d}{dy}\psi_{inc,2}^{TE/TM}(y)$ as output signals are obtained. The processor works equally for TE or TM polarisation.

has not yet been proposed. In addition, another resurgent challenge is creating a metasurface processor with an asymmetric response with respect to transverse momentum, namely one that distinguishes between $-k_t$ and k_t components of normally-incident beams. Such odd Optical Transfer Functions (OTFs) are needed for first order differentiation and edge detection [46, 47]. Indeed, among all mathematical operations, spatial differentiation is a fundamental mathematical operation used in many fields of science or engineering, and it is appealing for real-time image processing such as image sharpening and edge-based segmentation, with broad applications ranging from microscopy and medical imaging to industrial inspection and object detection [47].

In this paper, we design a Multiple-Inputs Multiple-Outputs (MIMO) computational metasurface for performing parallel optical processing with odd OTF on the transmission operational mode at normal beam illumination. We propose and demonstrate a real time parallel polarization-insensitive metasurface computer which can act as first-order differentiation operator for both TE and TM states. Systematically speaking, here, we propose 2×2 MIMO first-order differentiation processor for both orthogonal polarizations. The inputs and outputs correspond to different beam amplitude variations along orthogonal directions for a given polarization and angle. Using GSTCs and susceptibility tensors, we show that the presence of normal susceptibility components is required for breaking the even transmission symmetry at normal illumination. Additionally, based on relationships between the structural symmetries of the meta-atoms and the corresponding symmetries of their angular scattering response, we propose a simple meta-atom with geometrical symmetry with respect to the $x=y$ line, that enables first-order derivation for both input signals and both orthogonal polarizations. The waves transmitted

through the metasurface processor are then processed by simple Spatial Low Pass Filters (SLPFs) in order to extract and separate the output signal with x-variations from the one with y-variations. In order to demonstrate the concept, we provide a numerical example based on arbitrary input signals. The synthesized metasurface paves the path towards the implementation of MIMO spatial analog mathematical systems to accelerate optical signal and image processing routines.

II. GSTC AND META-ATOM DESIGN

The general concept of wave-based MIMO signal processing for normally incident beams is summarized in Fig. 1. We consider the case of a 2×2 MIMO first-order differentiation processor. Two distinct input signals, $\psi_{inc,1}^{TE/TM}(x)$ and $\psi_{inc,2}^{TE/TM}(y)$, with x- and y-variations, illuminate simultaneously the metasurface processor for a given (TE or TM) polarization. By properly designing the metasurface processor, the transmitted waves possess the same polarization as the input and contain a sum of their first-order differentiated signals. We then utilize two SLPF, along the k_x and k_y , to extract the desired output signals, namely $\frac{d}{dx}\psi_{inc,1}^{TE/TM}(x)$ and $\frac{d}{dy}\psi_{inc,2}^{TE/TM}(y)$. Theoretically speaking, we start from a reciprocal passive metasurface processor consisting of a periodic and homogeneous array of polarizable meta-atoms in the $z = 0$ plane, which acts as a two-dimensional electromagnetic discontinuity on the incident field created by external sources (see Figs. 2). Throughout the paper, we will assume a time-harmonic dependence of the form $e^{j\omega t}$, where $j^2 = -1$ is the imaginary unit.

A metasurface, described by a set of surface susceptibility components ($\bar{\chi}_{ee}, \bar{\chi}_{em}, \bar{\chi}_{me}, \bar{\chi}_{mm}$), can generate output fields with the desired transverse spatial depen-

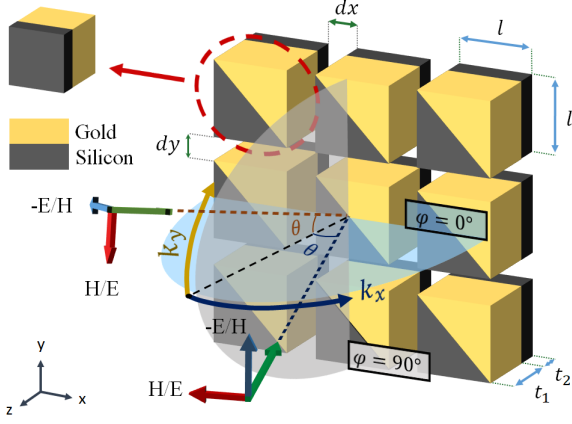


FIG. 2: Realization of the MIMO metasurface computer at an optical wavelength $\lambda_0 = 48.935\mu\text{m}$. The schematic shows an array of designed meta-atoms in the x-y plane.

The metasurface is excited by TM or TE-polarized electromagnetic waves. The geometrical parameters are $dx = dy = 4\mu\text{m}$, $l = 15\mu\text{m}$, $t_1 = 11\mu\text{m}$ and $t_2 = 4\mu\text{m}$.

gency of $\psi_{\text{ref/trans}}^{\text{TE/TM}}(x, y)$ in transmission/reflection mode when arbitrary input fields having the spatial dependence $\psi_{\text{inc}}^{\text{TE/TM}}(x, y)$ excite it. In fact, $\psi_{\text{inc}}^{\text{TE/TM}}(x, y)$ and $\psi_{\text{ref/trans}}^{\text{TE/TM}}(x, y)$ can be considered as the input and output signals of our linear system, where, the angular EM response of the metasurface processor determines the corresponding OTF, $O(k_x, k_y)$, in the spatial Fourier domain. Actually, the OTF represents the response to plane waves at different angles of incidence, providing a useful representation of the properties of optical metasurfaces [22].

Here, the solutions can be computed by $\psi_{\text{ref/trans}}(x, y) = F^{-1} \left[\bar{O}(k_x, k_y) \times F(\psi_{\text{inc}}(x, y)) \right]$ in which F and F^{-1} represent the operation of Fourier and inverse Fourier transform, respectively, and k_x and k_y denote the spatial frequency variable in the Fourier space. Commonly, the OTF provided by an array of polarizable meta-atoms has a tensorial format for both orthogonal polarizations which can be written as

$$\bar{O}^{\text{TE/TM}}(k_x, k_y) \equiv \begin{bmatrix} \tilde{u}^{\text{TE/TE}}(k_x, k_y) & \tilde{u}^{\text{TE/TM}}(k_x, k_y) \\ \tilde{u}^{\text{TM/TE}}(k_x, k_y) & \tilde{u}^{\text{TM/TM}}(k_x, k_y) \end{bmatrix} \quad (1)$$

where $\tilde{u}(k_x, k_y)$ refers to the functionality of the reflection (R) or transmission (T) coefficient of the metasurface processor from the incident wave angle. The first and second superscripts also represent the polarization of the input and output waves, respectively. The spatial OTF belonging to the metasurface computer can be extracted using the GSTCs formalism in which the meta-

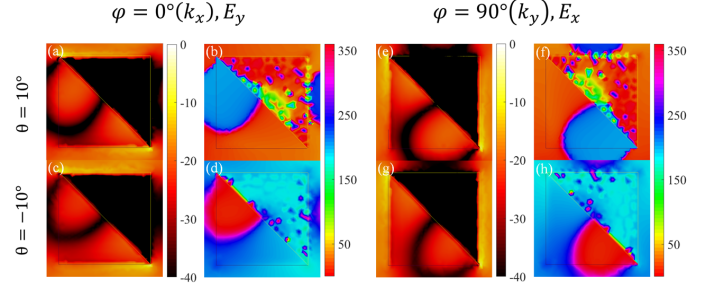


FIG. 3: Electric field profiles at plane $z = 0$ (top surface of meta-atoms) when $\theta = 10^\circ$ and -10° . (a), (c), (e) and (g) are amplitude of electric fields for $\theta = 10^\circ$ and -10° . Similarly, other plots contain phase information of electric fields.

surface transition conditions read [32, 48–51]

$$\hat{z} \times \Delta \mathbf{H} = j\omega \mathbf{P}_{\parallel} - \hat{z} \times \nabla_{\parallel} \mathbf{M}_z \quad (2)$$

$$\Delta \mathbf{E} \times \hat{z} = j\omega \mu \mathbf{M}_{\parallel} - \nabla_{\parallel} \left(\frac{\mathbf{P}_z}{\epsilon_0} \right) \times \hat{z} \quad (3)$$

in which, $\Delta \mathbf{E}$ and $\Delta \mathbf{H}$ are the difference of the electric and magnetic fields on both sides of the metasurface, respectively. \mathbf{P} and \mathbf{M} represent the electric and magnetic polarization densities induced on the metasurface. The susceptibility tensor components relate the polarization densities to the average electric and magnetic fields on both sides of the metasurface processor as $\mathbf{P} = \epsilon_0 \bar{\chi}_{ee} \mathbf{E}_{\text{av}} + \bar{\chi}_{em} \sqrt{\mu_0 \epsilon_0} \mathbf{H}_{\text{av}}$ and $\mathbf{M} = \bar{\chi}_{mm} \mathbf{H}_{\text{av}} + \bar{\chi}_{me} \sqrt{\frac{\epsilon_0}{\mu_0}} \mathbf{E}_{\text{av}}$, Here, ϵ_0 and η_0 are the permittivity and the characteristic impedance of free-space, respectively. In the most general case, each susceptibility tensor appearing in Equations. (2) and (3) include both longitudinal and tangential components, i.e. 36 susceptibilities. As we see in Equations. (2) and (3) if we consider a homogeneous metasurface without normal polarization ($P_z = M_z = 0$), only purely tangential polarizations exist, and no asymmetric function with respect to x-coordinate (k_x for example) is allowed. In fact, in this circumstance, the synthesized OTF has an even response (k_x^2 for example) respect to x-coordinate. However, when we involve the P_z and M_z terms, according to Equations. (2) and (3), the $\partial_x = jk_x$ (or $\partial_y = jk_y$) operators in $\nabla_{\parallel}(\cdot)$ make a spatial asymmetric OTF possible. To delve more into it and have an better awareness of how the angular scattering response of a metasurface depends on its normal susceptibilities, we begin the study with a simplified but pertinent scenario. We synthesize the metasurface processor with an expected performance described by an OTF specified on $(k_x, 0)$ and $(0, k_y)$. For brevity and avoiding the complexity of relations, we will write the relations, Reflection and Transmission of metasurface, only for $(k_x, 0)$. Naturally, a similar procedure

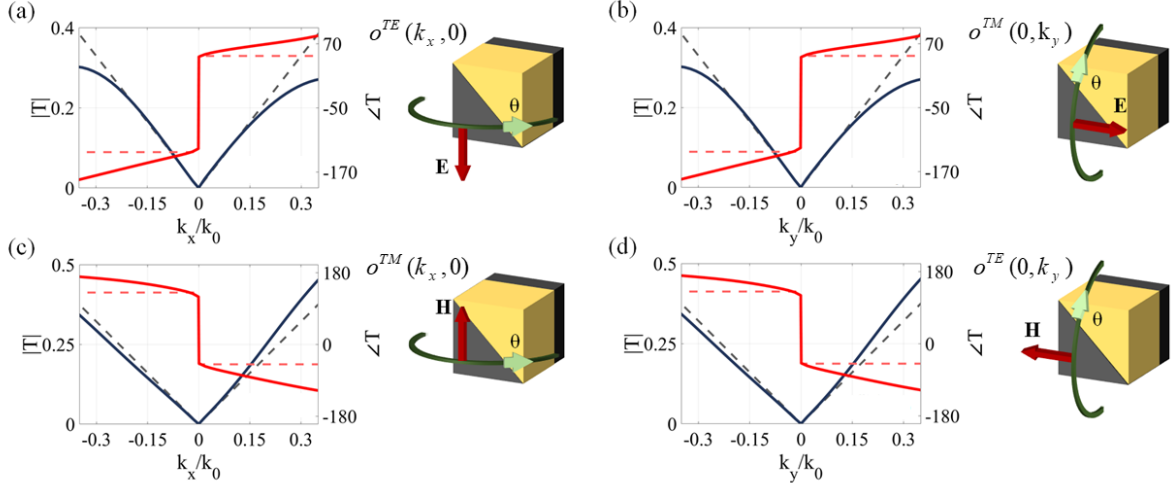


FIG. 4: Synthesized OTF. (a) and (c) The amplitude (black) and phase (red) of the synthesized $\text{OTF}(k_x, 0)$ associated with the first-order differentiation realized by the metasurface processor for TE and TM polarization, respectively. Also, (b) and (d) are similar plots for $\text{OTF}(0, k_y)$. The synthesized and ideal OTFs are indicated with solid and dashed lines, respectively.

can be mimicked for $(0, k_y)$. Without loss of generality, we focus on TM-polarized illumination. Keeping the polarization preservation criterion in mind, the susceptibility components that may be excited in our case are

$$\bar{\bar{\chi}}_{ee} = \begin{pmatrix} \chi_{ee}^{xx} & 0 & \chi_{ee}^{xz} \\ 0 & 0 & 0 \\ \chi_{ee}^{zx} & 0 & \chi_{ee}^{zz} \end{pmatrix}, \quad \bar{\bar{\chi}}_{mm} = \begin{pmatrix} 0 & 0 & 0 \\ 0 & \chi_{mm}^{yy} & 0 \\ 0 & 0 & 0 \end{pmatrix} \quad (4)$$

The reciprocity conditions enforce $\bar{\bar{\chi}}_{ee}^T = \bar{\bar{\chi}}_{ee}$, $\bar{\bar{\chi}}_{mm}^T = \bar{\bar{\chi}}_{mm}$. In this case, the reflection and transmission coefficients can be expressed in terms of the metasurface susceptibilities as shown in [32], and are given by

$$\gamma = 2[k_z^2 \chi_{ee}^{xx} + k_x^2 \chi_{ee}^{zz} + k_0^2 \chi_{mm}^{yy}] + k_0^2 (\chi_{ee}^{xx} \chi_{mm}^{yy}) - jk_z [k_x^2 (\chi_{ee}^{xz} - \chi_{ee}^{zx}) + 4]. \quad (5)$$

$$\mathbf{T}(k_x, 0) = \frac{jk_z}{\gamma} \{k_x^2 (\chi_{ee}^{xz} - \chi_{ee}^{zx}) - 4 + 4jk_x \chi_{ee}^{xz} - k_0^2 \chi_{ee}^{yy} \chi_{mm}^{xx}\}. \quad (6)$$

$$\mathbf{R}(k_x, 0) = \frac{2}{\gamma} \{k_x^2 \chi_{ee}^{zz} - k_z^2 \chi_{ee}^{xx} + k_0^2 \chi_{mm}^{yy}\}. \quad (7)$$

As can be noticed from Equations. (5) and (6), the presence of non-zero χ_{ee}^{xz} component makes the transmission transfer function odd with respect to the k_x variable, creating an asymmetric function of θ . The other normal susceptibility components cannot be used to break the angular symmetry of the transmission transfer function, e.g. χ_{ee}^{zz} induces a term proportional to k_x^2 in the relations, which implies an even-symmetric function of θ . We conclude that the normal polarizability component χ_{ee}^{xz} is mandatory for breaking the angular symmetry of the transmission of the metasurface.

From a realization point of view, there are fruitful relationships between the structural symmetries of the metasurface scattering meta-atoms and the corresponding symmetries of their angular scattering response. Geometrically, three types of symmetries are conceivable for the constituent meta-atoms: a reflection symmetry through the z -axis (σ_z), a 180° -rotation symmetry around the y -axis (C_2), and a reflection symmetry through the x -axis (σ_x) [32]. Regarding a reciprocal metasurface, the angular spectrum of the reflection coefficient exposes a σ_z symmetry, while that of the transmission coefficient has a C_2 symmetry. Most importantly, a metasurface with both normal and tangential susceptibilities are macroscopically achieved when the occupying meta-atoms do not microscopically render any geometrical symmetry.

In fact, when the meta-atoms are deprived of mentioned geometrical symmetry the resultant metasurface will present χ_{ee}^{xz} (or χ_{ee}^{zx}). Breaking both vertical and horizontal mirror symmetries of meta-atom is therefore required for realizing the asymmetric OTF response [32]. In this line of thought, we design an asymmetric meta-atom Fig. 2b comprising of two materials (gold [52] and silicon ($\epsilon_r = 12$)), for operation at $\lambda_0 = 48.935 \mu\text{m}$. The presented meta-atom would neither be σ_z symmetric nor C_2 symmetric. In fact, we break both vertical and horizontal mirror symmetries to enable a non-zero normal polarization, χ_{ee}^{xz} , reaching an asymmetric OTF.

Another important point about the structural symmetry of the designed meta-atom is that the meta-atom is symmetric respect to $x=y$ line. This symmetrical feature is of importance for reaching parallel optical signal computing. This point can be figured out from Fig. 3 which shows the amplitude and phase of electric field profiles at plane $z=0$ for both $\theta = 10^\circ$ and -10° . By comparing

the Fig. 3 a and b with Fig. 3 e and f, the symmetrical feature respect to $x=y$ line is obvious. In fact, as we expected, the mirror image of Fig. 3 a and b can be seen in Fig. 3 e and f. A similar discussion for Fig. 3 c and d and Fig. 3 g and h is valid. In summary, due to this geometrical symmetry, we expect effectively to attain the same transmission response in x and y directions which enables parallel optical signal processing.

In the following, we will demonstrate some possible wave-based functionalities that can be unlocked by the proposed metasurface processor, as the fundamental block realizing the operator of choice. One of the most important mathematical functions that has been less explored in the literature is the first-order differentiation operator whose spatial OTF can be written as $O(k_x, 0) = \alpha j k_x$ and $O(0, k_y) = \beta j k_y$, where α and β are complex constant coefficients which represent the gain values of the first-order differentiation operators.

Fig. 4 displays the synthesized and required OTF for transmitting the first-order derivation of the input field-profile for both TE and TM polarizations. The structural specifications of the meta-atom leads to resonance for normal incident waves ($k_x = k_0$). As we can see in Fig. 4, the amplitude of the transmission coefficient is infinitesimal at the normal incident angle and it linearly increases when the incident angle changes. The 180 phase difference degrees between $k_t > 0$ and $k_t < 0$ of OTF indicates asymmetric, odd, angular response of OTF. The results are simulated using CST full-wave commercial software.

Here, as we discussed above, the geometry of the proposed meta-atom enables us to have a same synthesized OTF for y directions which is important for our goal (see Fig. 4). The proposed meta-atom can elaborately mimic the required k_x and k_y -dependency of first-order differentiator (see Fig. 4). The phase and amplitude of the resulting transmission coefficient are plotted for both orthogonal polarizations in Figs. 4 a-d. An excellent agreement between the synthesized OTF and the exact OTF has been achieved as long as the normalized spectral beamwidth of the input signals lies within $|W/k_0| < 0.35$. As we can see in Fig.4, the values of α and β are $|\alpha| \approx |\beta| \approx 1$

Also, it is clear from electric field profile point of view which is plotted in Fig. 3; by comparing the Fig. 3 a and b with Fig. 3 c and d, as we expect, we see the same amplitude and 180 phase difference between the $\theta = 10^\circ$ and $\theta = -10^\circ$. The same discussion for Fig. 3 e and f and Fig. 3 g and h for $\phi = 90$ is valid.

III. REAL-TIME PARALLEL OPTICAL SIGNAL PROCESSING

In this section, we explore a 2×2 MIMO first-order differentiation processor, which enables independent parallel channels for signal processing, a key result of this paper.

Our final goal is performing the first-order differ-

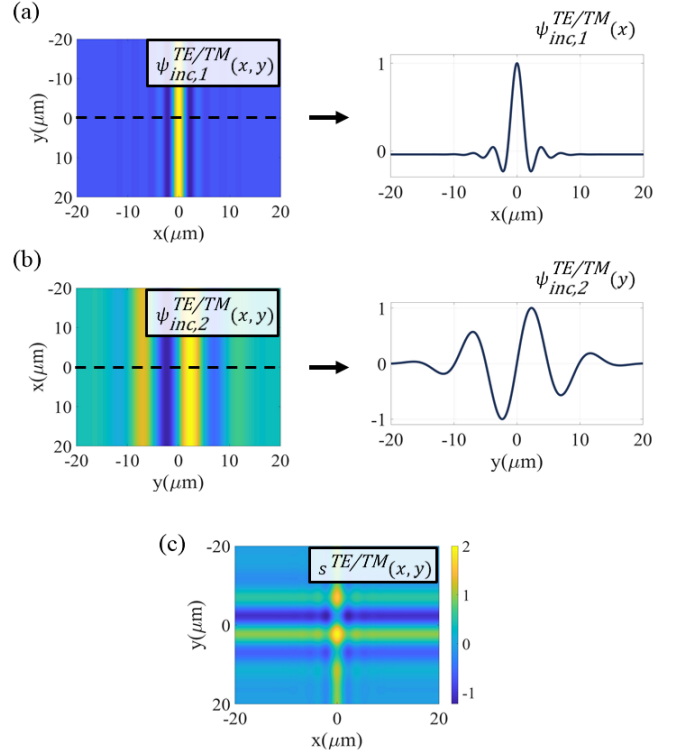


FIG. 5: Input signals. (a) and (b) The first and second arbitrary incident field profiles, respectively. (c) Combination of both input signals in x-y plane for both orthogonal polarization states.

entiation simultaneously on two distinct input signals, $\psi_{inc,1}^{TE/TM}(x)$ and $\psi_{inc,2}^{TE/TM}(y)$, regardless of the polarisation chosen (TE/TM means that we have the freedom to choose either TE or TM polarisation). In fact, we start from a combination of two arbitrary input signals ($s^{TE/TM}(x, y) = \psi_{inc,1}^{TE/TM}(x) + \psi_{inc,2}^{TE/TM}(y)$) created by two sources, in which one of them has an x variation ($\psi_{inc,1}^{TE/TM}(x)$) and another one has a y variation ($\psi_{inc,2}^{TE/TM}(y)$). Therefore, by using a Fourier Transform, we can theoretically write

$$S^{TE/TM}(k_x, k_y) = \Psi_{inc,1}^{TE/TM}(k_x)\delta(k_y) + \Psi_{inc,2}^{TE/TM}(k_y)\delta(k_x) \quad (8)$$

where $S^{TE/TM}(k_x, k_y)$ is the combination of two input signals in Fourier domain and $\delta(\cdot)$ is Delta Dirac function. Based on the synthesized OTF (see Fig. 4), the two-dimensional $O^{TE/TM}(k_x, k_y)$ can be written as follow

$$O^{TE/TM}(k_x, k_y) = \begin{cases} \alpha j k_x & k_y = 0 \\ \beta j k_y & k_x = 0 \\ W(k_x, k_y) & k_x, k_y \neq 0 \end{cases} \quad (9)$$

where $W(k_x, k_y)$ is corresponding to the synthesized OTF at $(k_x, k_y \neq 0)$. As we mentioned before, due to the fact that our input signals only have x or y variations,

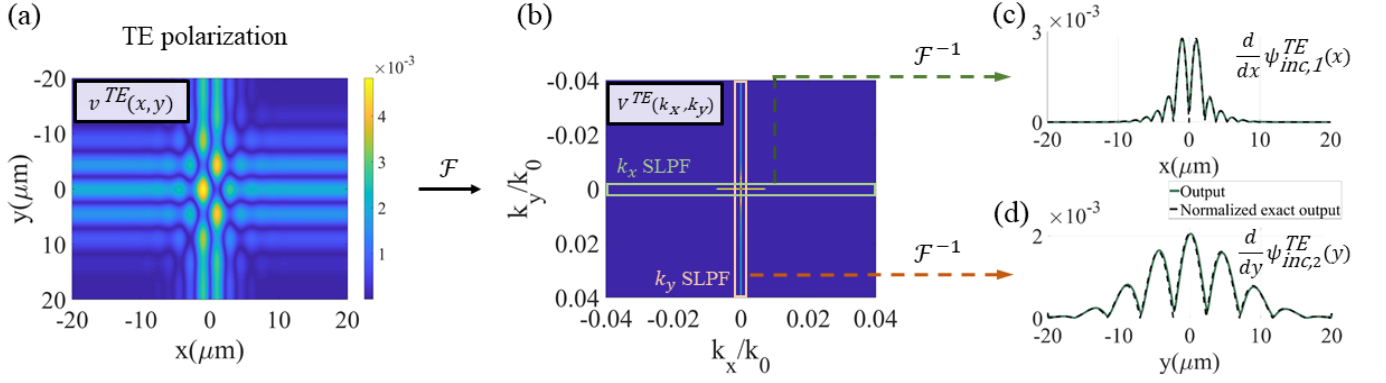


FIG. 6: Output signals. The TE-polarized transmitted image in space domain (a) and in Fourier domain (b). (c) and (d) are extracted output signals after passing from k_x -SLPF and k_y -SLPF, respectively.

the synthesized OTF associated with metasurface processor needs to have the first-order differentiator function only in $(k_x, 0)$ and $(0, k_y)$. Therefore, the expression for $W(k_x, k_y)$ is unimportant for our purpose. By multiplying the OTF to the $S^{\text{TE/TM}}(k_x, k_y)$, the output $V(k_x, k_y)$ can be written as follow

$$V(k_x, k_y) = O^{\text{TE/TM}}(k_x, k_y)S^{\text{TE/TM}}(k_x, k_y) \quad (10)$$

$$= \begin{cases} \alpha j k_x \Psi_{\text{inc},1}^{\text{TE/TM}}(k_x) \delta(k_y) \\ + \alpha j k_x \Psi_{\text{inc},2}^{\text{TE/TM}}(k_y) \delta(k_x) & k_y = 0 \\ \beta j k_y \Psi_{\text{inc},1}^{\text{TE/TM}}(k_x) \delta(k_y) \\ + \beta j k_y \Psi_{\text{inc},2}^{\text{TE/TM}}(k_y) \delta(k_x) & k_x = 0 \\ 0 & k_x, k_y \neq 0 \end{cases}$$

Based on the definition of delta Dirac function [53] and after some mathematical manipulations we have $V(k_x, k_y) = \alpha j k_x \Psi_{\text{inc},1}^{\text{TE/TM}}(k_x) \delta(k_y) + \beta j k_y \Psi_{\text{inc},2}^{\text{TE/TM}}(k_y) \delta(k_x)$; therefore, by using inverse Fourier Transform $v(x, y)$ can be written as follow [10, 17]

$$v(x, y) = \quad (11)$$

$$\int_{-\infty}^{+\infty} \int_{-\infty}^{+\infty} \alpha j k_x \Psi_{\text{inc},1}^{\text{TE/TM}}(k_x) \delta(k_y) e^{-jk_x x} e^{-jk_y y} dk_x dk_y \quad (12)$$

$$+ \int_{-\infty}^{+\infty} \int_{-\infty}^{+\infty} \beta j k_y \Psi_{\text{inc},2}^{\text{TE/TM}}(k_y) \delta(k_x) e^{-jk_x x} e^{-jk_y y} dk_x dk_y$$

$$= \alpha \frac{d}{dx} \psi_{\text{inc},1}^{\text{TE/TM}}(x) + \beta \frac{d}{dy} \psi_{\text{inc},2}^{\text{TE/TM}}(y)$$

Finally, by using two SLPFs, we can extract and separate our desired output signals as following

$$k_y\text{-SPLF}\{v(x, y)\} = \alpha \frac{d}{dx} \psi_{\text{inc},1}^{\text{TE/TM}}(x) \quad (13)$$

$$k_x\text{-SPLF}\{v(x, y)\} = \beta \frac{d}{dy} \psi_{\text{inc},2}^{\text{TE/TM}}(y) \quad (14)$$

Conceptually, the schematic sketch of the 2×2 MIMO first-order differentiation processor is shown in Fig. 1b. Consider a computational and realistic scenario in which two different input signals in x and y directions ($\psi_{\text{inc},1}^{\text{TE/TM}}(x)$ and $\psi_{\text{inc},2}^{\text{TE/TM}}(y)$) collide to a reciprocal metasurface from normal direction. Upon interacting with the metasurface computer and depending on the k_t -modulation of the spatial OTF dictated by array of asymmetric meta-atoms, the combination of input signals ($s^{\text{TE/TM}}(x, y)$) is mapped along k_x and k_y directions of output signal ($V^{\text{TE/TM}}(k_x, k_y)$) in Fourier domain (see Equation.10). Thereafter, desired output signals ($\frac{d}{dx} \psi_{\text{inc},1}^{\text{TE/TM}}(x)$ and $\frac{d}{dy} \psi_{\text{inc},2}^{\text{TE/TM}}(y)$) can be obtained and separated after passing from Spatial Low-Pass Filters (SLPF).

To demonstrate the real-time parallel computing capability of the proposed scheme, we consider as inputs the two arbitrary signals shown in Fig. 5a and b. Simultaneously emitted by two sources, they combine into the two-dimensional function shown in Fig. 5c. This field illuminates the metasurface computer, which generates the output image ($v^{\text{TE/TM}}(x, y)$) (see Figs. 6a and 7a). Consistent with our design, the $V^{\text{TE/TM}}(k_x, k_y)$ image only has values along k_x and k_y directions (see Figs. 6b and 7b and Equation. 10). Subsequently, by using the SLPFs along k_x and k_y , the final output signals are generated and shown in Figs. 6 and 7, for TE and TM polarizations, respectively. One should note that many prior arts have introduced designs for appropriate SLPF based on a simple single metasurface [11, 54, 55]. The extraction performance of desired output signals depend on these SLPFs. Actually, the sharper the SLPFs, the better the extraction and separation performance. For this reason, we cascade two first-order integrator metasurface based on [55] to reach sharp-SLPFs. The transmission coefficients of desired SLPF are shown in Fig.8. For the sake of comparison, Figs. 6c and d and Figs. 7c and d also plots the exact and the output signals for both orthogonal polarizations. An excellent agreement between simulated and benchmark results has been achieved when

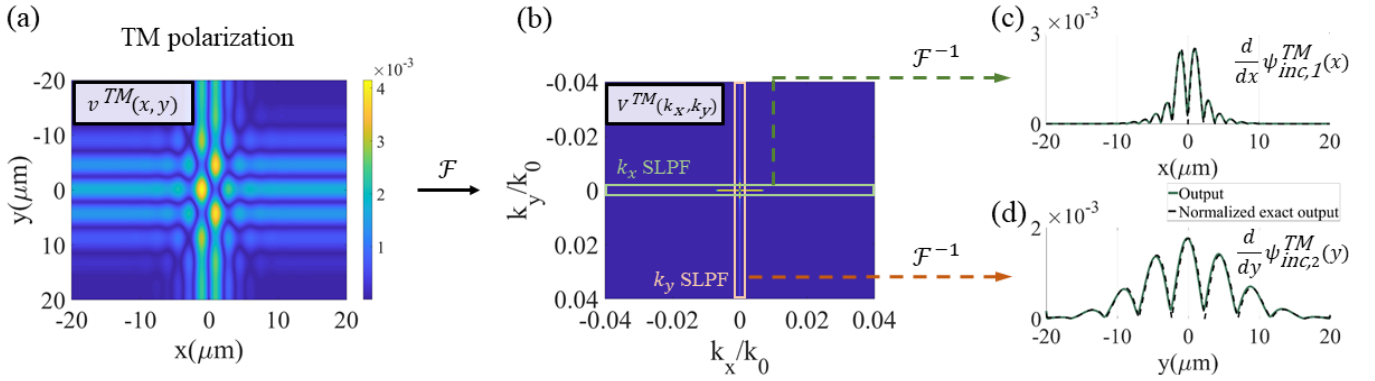


FIG. 7: Output signals. TM-polarized transmitted image in space domain (a) and in Fourier domain (b). (c) and (d) are extracted output signals after passing from k_x -SLPF and k_y -SLPF, respectively.

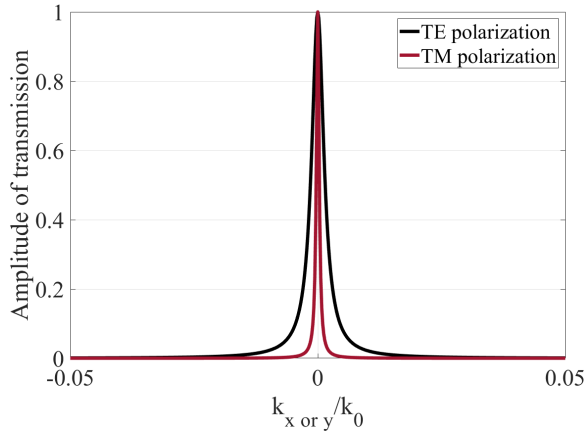


FIG. 8: Transmission coefficients of k_x - k_y -SLPF for both TE and TM states.

the normalized spectral beamwidth of the input signals lies within $|W| < 0.35k_0$.

IV. CONCLUSION

In summary, a 2×2 MIMO first-order differentiation processor was elaborately designed to be utilized in a spatial analog computing platform for reaching massively parallel processing. Through synthesizing proper asymmetric meta-atom, based on GSTC and susceptibility tensors, the metasurface computer is empowered to realize the required phases and amplitudes of the OTF associated with the first-order differentiation operation. This novel optical MIMO metasurface processor with asymmetric optical response can perform spatial differentiation on two distinct input signals (in x and y directions) at the same time for both orthogonal polarization states. The proposed theoretical framework foretastes that the presented design overcomes the substantial restrictions imposed by previous investigations such as large architectures arising from the need of additional subblocks, slow responses, and most importantly, supporting only one/single input and certain incident polarization. The numerical results prove that the proposed metasurface computer may be thought of as an efficient and flexible host for being utilized in the field of real-time parallel optical signal processing.

- [1] J. Nakamura, (2005).
- [2] J. W. Goodman, Introduction to Fourier optics, 3rd ed., by JW Goodman. Englewood, CO: Roberts & Co. Publishers, 2005 1 (2005).
- [3] H. Stark, (1982).
- [4] C. Goodman, Art Journal **49**, 248 (1990).
- [5] A. Silva, F. Monticone, G. Castaldi, V. Galdi, A. Alù, and N. Engheta, Science **343**, 160 (2014).
- [6] D. R. Solli and B. Jalali, Nature Photonics **9**, 704 (2015).
- [7] S. Abdollahramezani, A. Chizari, A. E. Dorche, M. V. Jamali, and J. A. Salehi, Optics letters **42**, 1197 (2017).
- [8] H. Babashah, Z. Kavehshah, S. Koohi, and A. Khavasi, J. Opt. Soc. Am. B **34**, 1270 (2017).
- [9] A. Pors, M. G. Nielsen, and S. I. Bozhevolnyi, Nano letters **15**, 791 (2015).
- [10] A. Youssefi, F. Zangeneh-Nejad, S. Abdollahramezani, and A. Khavasi, Opt. Lett. **41**, 3467 (2016).
- [11] H. Kwon, D. Sounas, A. Cordaro, A. Polman, and A. Alù, Phys. Rev. Lett. **121**, 173004 (2018).
- [12] Optics Communications **407**, 338 (2018).
- [13] A. Momeni, H. Rajabalipanah, A. Abdolali, and K. Achouri, Phys. Rev. Applied **11**, 064042 (2019).
- [14] F. Zangeneh-Nejad and R. Fleury, Nature Communications **10** (2019), 10.1038/s41467-019-10086-3.
- [15] A. Abdolali, A. Momeni, H. Rajabalipanah, and K. Achouri, New Journal Of Physics **21**, 113048 (2019).

- [16] T. Zhu, Y. Lou, Y. Zhou, J. Zhang, J. Huang, Y. Li, H. Luo, S. Wen, S. Zhu, Q. Gong, M. Qiu, and Z. Ruan, *Phys. Rev. Applied* **11**, 034043 (2019).
- [17] T. Zhu, Y. Zhou, Y. Lou, H. Ye, M. Qiu, Z. Ruan, and S. Fan, *Nature Communications* **8** (2017), 10.1038/ncomms15391.
- [18] *Optics Communications* **458**, 124674 (2020).
- [19] A. Cordaro, H. Kwon, D. Sounas, A. F. Koenderink, A. Al, and A. Polman, *Nano Letters* **19**, 8418 (2019).
- [20] Y. Zhou, W. Wu, R. Chen, W. Chen, R. Chen, and Y. Ma, *Advanced Optical Materials* **8**, 1901523 (2020).
- [21] N. Mohammadi Estakhri, B. Edwards, and N. Engheta, *Science* **363**, 1333 (2019).
- [22] T. J. Davis, F. Eftekhari, D. E. Gómez, and A. Roberts, *Phys. Rev. Lett.* **123**, 013901 (2019).
- [23] C. Guo, M. Xiao, M. Minkov, Y. Shi, and S. Fan, *Optica* **5**, 251 (2018).
- [24] Z. Wang, T. Li, A. Soman, D. Mao, T. Kananen, and T. Gu, *Nature communications* **10**, 3547 (2019).
- [25] P. Karimi, A. Khavasi, and S. S. M. Khaleghi, *Opt. Express* **28**, 898 (2020).
- [26] J. Zhou, H. Qian, C.-F. Chen, J. Zhao, G. Li, Q. Wu, H. Luo, S. Wen, and Z. Liu, *Proceedings of the National Academy of Sciences* **116**, 11137 (2019).
- [27] H. Rajabalipanah, A. Abdolali, S. Iqbal, L. Zhang, and T. J. Cui, (2020), arXiv:2002.06773 [physics.app-ph].
- [28] N. Yu and F. Capasso, *Nature materials* **13** **2**, 139 (2014).
- [29] N. Yu, P. Genevet, M. A. Kats, F. Aieta, J.-P. Tetienne, F. Capasso, and Z. Gaburro, *Science* **334**, 333 (2011).
- [30] S. Sun, K.-Y. Yang, C.-M. Wang, T.-K. Juan, W. T. Chen, C. Y. Liao, Q. He, S. Xiao, W.-T. Kung, G.-Y. Guo, L. Zhou, and D. P. Tsai, *Nano Letters* **12**, 6223 (2012), pMID: 23189928.
- [31] A. V. Kildishev, A. Boltasseva, and V. M. Shalaev, *Science* **339** (2013), 10.1126/science.1232009.
- [32] K. Achouri and O. J. F. Martin, *IEEE Transactions on Antennas and Propagation* **68**, 432 (2020).
- [33] A. Momeni, M. Safari, A. Abdolali, and N. P. Kherani, “Tunable and dynamic polarizability tensor for asymmetric metal-dielectric meta-cylinders,” (2019), arXiv:1904.04102 [physics.app-ph].
- [34] K. Rouhi, H. Rajabalipanah, and A. Abdolali, *Carbon* **149**, 125 (2019).
- [35] I. Shahid, H. Rajabalipanah, L. Zhang, X. Qiang, A. Abdolali, and T. J. Cui, *Nanophotonics* **9**, 703 (2020), 3.
- [36] M. Kiani, M. Tayarani, A. Momeni, H. Rajabalipanah, and A. Abdolali, *Opt. Express* **28**, 5410 (2020).
- [37] K. Rouhi, H. Rajabalipanah, and A. Abdolali, *Annalen der Physik* **530**, 1700310 (2018).
- [38] H. Rajabalipanah, A. Abdolali, J. Shabanpour, A. Momeni, and A. Cheldavi, *ACS Omega* **4**, 14340 (2019).
- [39] S. E. Hosseinijad, K. Rouhi, M. Neshat, R. Farajidana, A. Cabellos-Aparicio, S. Abadal, and E. Alarcón, *Scientific Reports*, (2019).
- [40] R. Kargar, K. Rouhi, and A. Abdolali, *Optics Communications* **462**, 125331 (2020).
- [41] A. Momeni, K. Rouhi, H. Rajabalipanah, and A. Abdolali, *Scientific Reports* **8** (2018), 10.1038/s41598-018-24553-2.
- [42] S. E. Hosseinijad, K. Rouhi, M. Neshat, A. Cabellos-Aparicio, S. Abadal, and E. Alarcón, *IEEE Transactions on Nanotechnology* **18**, 734 (2019).
- [43] M. M. Moeini, H. Oraizi, and A. Amini, *Phys. Rev. Applied* **11**, 044006 (2019).
- [44] M. Movahhedi, M. Karimipour, and N. Komjani, *IEEE Antennas and Wireless Propagation Letters* **18**, 1507 (2019).
- [45] M. M. Moeini, H. Oraizi, A. Amini, and V. Nayyeri, *Scientific Reports* **9** (2019).
- [46] J. Canny, *IEEE Transactions on Pattern Analysis and Machine Intelligence* **PAMI-8**, 679 (1986).
- [47] D. Marr, E. Hildreth, and S. Brenner, *Proceedings of the Royal Society of London. Series B. Biological Sciences* **207**, 187 (1980).
- [48] K. Achouri, G. Lavigne, and C. Caloz, *Journal of Applied Physics* **120**, 235305 (2016).
- [49] K. Achouri and C. Caloz, *Nanophotonics* (2017).
- [50] Achouri, Karim, Khan, Bakthiar Ali, Gupta, Shulabh, Lavigne, Guillaume, Salem, Mohamed Ahmed, and Caloz, Christophe, *EPJ Applied Metamaterials* **2**, 12 (2015).
- [51] G. Lavigne, K. Achouri, V. S. Asadchy, S. A. Tretyakov, and C. Caloz, *IEEE Transactions on Antennas and Propagation* **66**, 1321 (2018).
- [52] E. D. Palik, (1998).
- [53] I. M. Gelfand and Shilov, Providence, Rhode Island : AMS Chelsea Publishing (2017).
- [54] A. Arbabi, Y. Horie, and A. Faraon, *Nature nanotechnology* **10** (2015).
- [55] F. Zangeneh-Nejad and A. Khavasi, *Optics letters* **42**, 1954 (2017).